INTERNATIONAL JOURNAL OF INNOVATIVE RESEARCH & DEVELOPMENT

ISSN: 2278 – 0211

A Novel Multilevel Inverter Topology For Induction Motor Drive

V.MATTHEW
M.Tech Student Scholar, Power Electronics & Drives, Department of Electrical &Electronics Engineering,Gudlavalleru Engineering College, Krishna, A.P, India
G.BALAJI
AssociateProfessor,Department of Electrical & Electronics Engineering,Gudlavalleru Engineering College, Krishna, A.P, India

Abstract:

This paper presents the simulation and implementation of multilevel inverter fed induction motor drive. The output harmonic content is reduced by using multilevel inverter. In symmetrical circuit, the voltage and power increase with the increase in the number of levels of inverter. The switching angle for the pulse is selected in such way to reduce the harmonic distortion. This drive system has advantages like reduced total harmonic distortion and higher torque. The model of the multilevel inverter system is developed with PWM strategy to control the induction motor. The rate of change of voltage with respect to time i.e. dv/dt is very high at these edges, of the order of 500–5000 V/μs.The two-level inverter topology has attracted attention in low power low voltage drive applications where as Three-Level inverter topology has attracted attention in high power High performances voltage drive applications. Single-phase VSI cover low-range power applications and three-phase VSI cover the medium- to high-power applications. The Main purpose of these three level inverter topologies is to provide a three phase voltage source, where the amplitude, phase, and frequency of the voltages should always be controllable. Although most of the applications require sinusoidal voltage waveforms

Key words :*Medium-voltage ac drives, multilevel converter topologies.*

1.Introduction

Multilevel converters are considered for high-power medium-voltage drive applications, because the power structure can be realized with devices of lower voltage ratings [1]–[10]. A five-level inverter structure by cascading conventional two-level and three-level inverters is proposed in Part I of this paper [20]. An open-loop control scheme is presented in Part I to maintain dc-link capacitor voltage balancing and common-mode voltage (CMV) elimination in a dual five-level inverter-fed open-end winding induction motor (IM) drive, which effectively uses only the available redundant switching states of the inverter. It is pointed out that the proposed open loop controller is unable to take any corrective action to reduce the unbalance in the capacitor voltages that may arise.Every individual inverter is capable of generating three different voltage output +Vdc ,0, -Vdc by connecting the dc source to the ac output side by different combinations of the four switches S1 , S2 , S3 and S4 [1]. The synthesize ac output voltage waveform of the sum of all the individual inverter's outputs. The number of output phase voltage level of cascade multilevel inverter is 2s+1 where S is the number of dc sources. This outstandingly increases the level number of the output wave form and thereby dramatically reduced to the low order harmonics and total harmonic distortion. One of the foremost motives for developing the multilevel inverter is to reduce costSimilar voltage profiles can also be obtained by using higher order neutral-point-clamped (NPC) multilevel inverters or by cascading a number of two-level inverters. However, the multilevel NPC inverters suffer from dc-bus imbalance, device underutilization problems and unequal ratings of the clamped diodes, etc., which are not very serious problems for inverters with three levels or lower. The capacitor voltage imbalance for a five-level one is presented in which suggest the need of extra hardware in the form of dc choppers or a back-to-back connection of multilevel converters. The cascaded H-bridge topology suffers from the drawbacks of the usage of huge dc-bus capacitors and complex input transformers for isolated dc bus for each module. These drawbacks are addressed in the proposed topology. Furthermore, the power circuit is modular in structure, and hence, the number of modules to be connected in series depends on the power of the drive.

2.Proposed Converter Topology

The proposed general configuration of "n" number of three level inverters connected in series is shown in Fig. 1. Each inverter module is a three-phase NPC three-level inverter. At the output stage, transformers are used to have the series connection of three-level

inverters, as shown in Fig. 1. If "Vdc" is the dc-bus voltage of each inverter module, then "α" is the turns ratio of each transformer and "n" is the number of inverter modules then for sine PWM (SPWM) strategy; the motor rms phase voltage (VPh_motor) can be expressed as follows

Rms of Vph_motor =√3 αmnV_dc/(2√2)

Where m is the modulation index of the inverter topology

defined as follows

m=(Peak of V_(ph_inverter))/(n V_dc/2)

Vph_inverter is the total phase voltage reference of the inverter

topology. For the given peak of VPh_motor, peak of Vph_inverter

can be computed as follows

Peak of V_(ph_inverter)=(Peak of V_(ph_motor))/(√3 α)

The generation of individual reference voltage signal of each inverter is discussed as follows.

The gate pulses for each three-level inverter module can be derived using two carrier signals. Thus, "n" numbers of such three-level inverter modules require "2n" number of carriers [10], [13]. The three-phase voltage reference signals are then compared with these carrier waves to produce the gate pulses for the inverters. For example, the carrier waves and the sinusoidal modulating voltage signal (SPWM technique) for R phase is shown in Fig. 2 for four series-connected three-level inverters. The carrier waves 1 and 1_ (Fig. 2) with R-phase voltage reference controls the inverter module 1. Similarly, 2 2_, 3–3_, and 4–4_ carrier waves with R-phase voltage reference generate the gate pulses for the three-level inverter modules 2, 3, and 4, respectively. Thus, each inverter module produces the voltage proportional to a part of the reference phase voltage signals. It is important to note that no two three-level inverter modules switch simultaneously. Thus, the maximum dv/dt rate of the output voltage of this topology is limited to that of a single three-level inverter module. The references of each inverter are shown in Fig. 3. The corresponding output line voltages of each inverter are shown in Fig. 4. The four windings, one from each transformer, are connected in series and produced the net R-phase voltage, as shown in Fig. 5 Similarly, the other two phase voltages are generated.

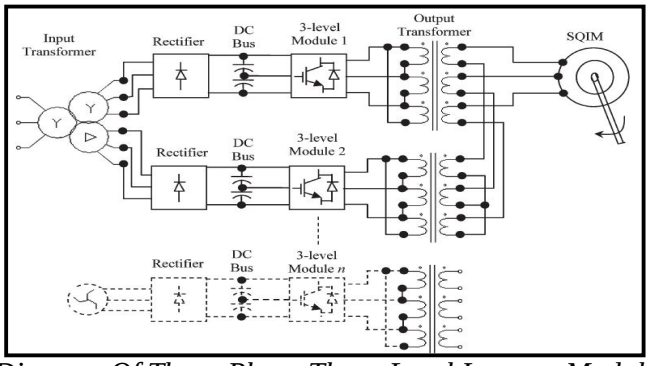

Figure1:Block Diagram Of Three-Phase Three-Level Inverter Modules Connected In Series Driving An Sqim

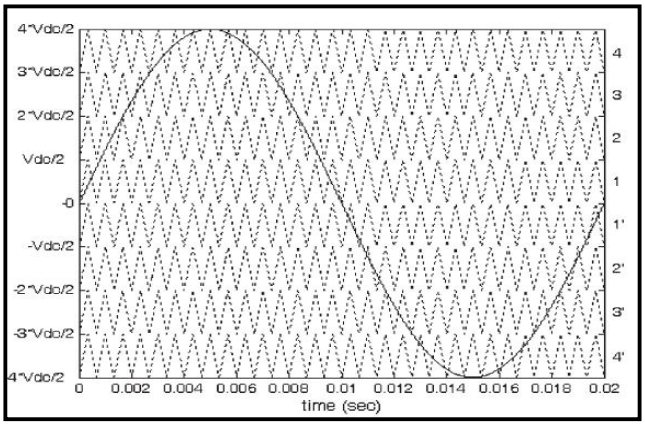

Figure2:Carrier Waves And The Sinusoidal Modulating Voltage Signal For R Phase In SPWM Technique

The line voltage spectra of individual inverters are shown in Fig. 4 for switching frequency of 2.5 kHz. These line voltages get added to produce the net phase voltage of the topology. The voltage spectra are expressed as a percentage of the maximum total fundamental (*V*peak) that can be produced by the topology.

$$V\_peak=\sqrt{2}*V\_(ph\_motor)$$

or *V*peak = 2078.5 V for *V*dc = 600 V, n = 4, α = 1, and m = 1 using (1). Hence, the spectra show the percentage share of the fundamental of each inverter module. These spectra also suggest that the line voltages of all these inverters contain additional small amount of the 5th-, 7th-, 11th-, 13th-, and higher order harmonics besides the normal switching harmonics. However, the net phase voltage and line voltage of this topology do not contain any of these harmonics, as suggested by the spectra shown in Fig. 5. These harmonics get canceled when the line voltages of the individual inverters are added by the transformers to produce the net phase voltages. The increased number of

steps in the motor terminal voltage reduces the *dv/dt* as that compared with a conventional two-level inverter.

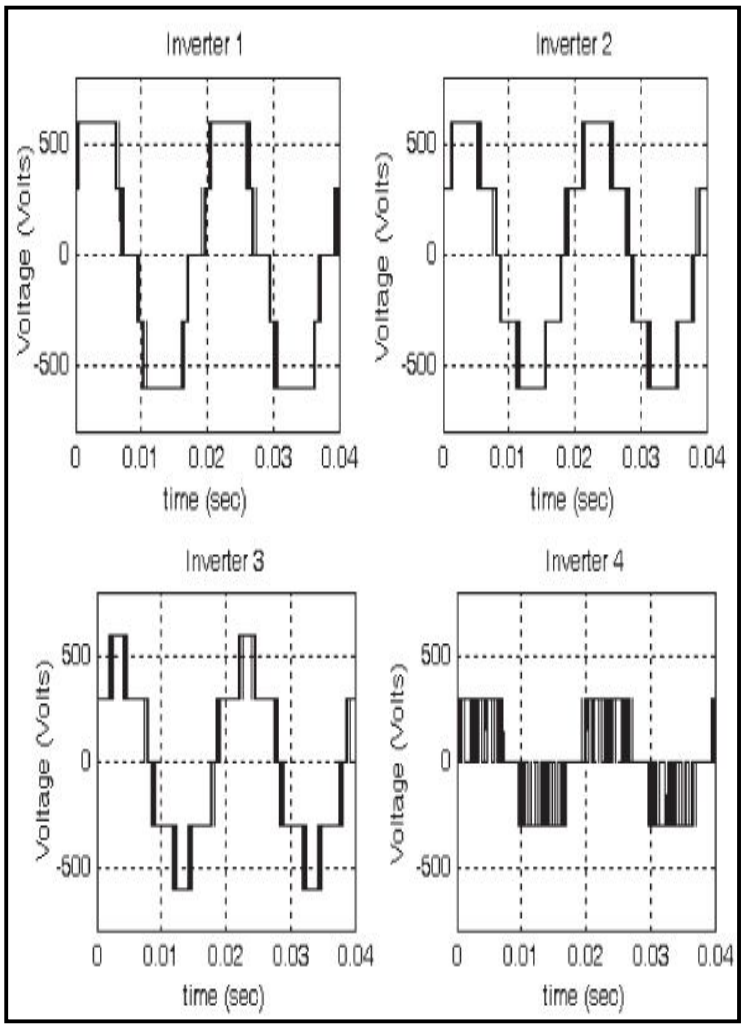

Figure3:Four Series Connected Inverters Individual Voltages

2.1.Dynamic Model Of Induction Motor

The induction machine d-q or dynamic equivalent circuit is shown in Fig. 1 and 2. One of the most popular induction motor models derived from this equivalent circuit is Krause's model detailed in [5]. According to his model, the modeling equations in flux linkage form are as follows:

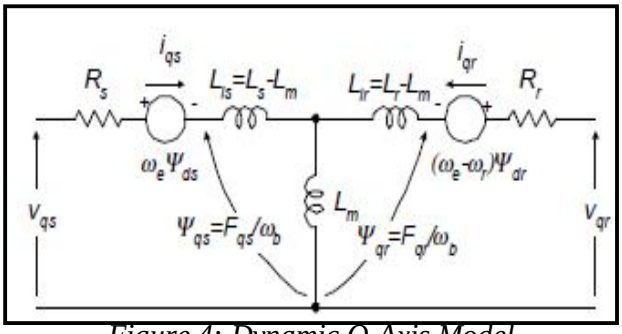

Figure 4: Dynamic Q-Axis Model

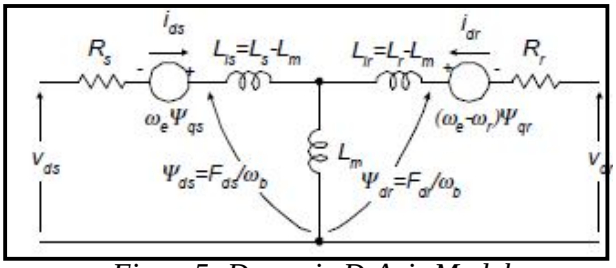

Figure5: Dynamic D-Axis Model

$$\frac{dF_{qs}}{dt}=\omega_b\left[v_{qs}-\frac{\omega_e}{\omega_b}F_{ds}+\frac{R_s}{x_{ls}}\left(F_{mq}+F_{qs}\right)\right] \quad (1)$$

$$\frac{dF_{ds}}{dt}=\omega_b\left[v_{ds}+\frac{\omega_e}{\omega_b}F_{qs}+\frac{R_s}{x_{ls}}\left(F_{md}+F_{ds}\right)\right] \quad (2)$$

$$\frac{dF_{qr}}{dt}=\omega_b\left[v_{qr}-\frac{\left(\omega_e-\omega_r\right)}{\omega_b}F_{dr}+\frac{R_r}{x_{lr}}\left(F_{mq}-F_{qr}\right)\right] \quad (3)$$

$$\frac{dF_{dr}}{dt}=\omega_b\left[v_{dr}+\frac{\left(\omega_e-\omega_r\right)}{\omega_b}F_{qr}+\frac{R_r}{x_{lr}}\left(F_{md}-F_{dr}\right)\right] \quad (4)$$

$$F_{mq}=x_{ml}^{*}\left[\frac{F_{qs}}{x_{ls}}+\frac{F_{qr}}{x_{lr}}\right] \quad (5)$$

$$F_{md}=x_{ml}^{*}\left[\frac{F_{ds}}{x_{ls}}+\frac{F_{dr}}{x_{lr}}\right] \quad (6)$$

$$i_{qs}=\frac{1}{x_{ls}}\left(F_{qs}-F_{mq}\right) \quad (7)$$

2.2 Voltage Source Converter (Vsc)

$$i_{ds} = \frac{1}{x_{ls}}\left(F_{ds} - F_{md}\right) \quad (8)$$

$$i_{qr} = \frac{1}{x_{lr}}\left(F_{qr} - F_{mq}\right) \quad (9)$$

$$i_{dr} = \frac{1}{x_{lr}}\left(F_{dr} - F_{md}\right) \quad (10)$$

$$T_e = \frac{3}{2}\left(\frac{p}{2}\right)\frac{1}{\omega_b}\left(F_{ds}i_{qs} - F_{qs}i_{ds}\right) \quad (11)$$

$$T_e - T_L = J\left(\frac{2}{p}\right)\frac{d\omega_r}{dt} \quad (12)$$

where d : direct axis,
q : quadrature axis,
s : stator variable,
r : rotor variable,
F_{ij} is the flux linkage (i=q or d and j=s or r),
v_{qs}, v_{ds} : q and d–axis stator voltages,
v_{qr}, v_{dr} : q and d–axis rotor voltages,
F_{mq},F_{md} : q and d axis magnetizing flux linkages,
Rr : rotor resistance,
Rs : stator resistance,
X_{ls} : stator leakage reactance ($\omega_e L_{ls}$),
X_{lr} : rotor leakage reactance ($\omega_e L_{lr}$),
X_{ml}^{*} : $1\Big/\left(\frac{1}{x_m}+\frac{1}{x_{ls}}+\frac{1}{x_{lr}}\right)$,
i_{qs}, i_{ds} : q and d–axis stator currents,
i_{qr}, i_{dr} : q and d–axis rotor currents,
p : number of poles,
J : moment of inertia,
T_e : electrical output torque,
T_L(or T_l) : load torque,
ω_e : stator angular electrical frequency,
ω_b : motor angular electrical base frequency,
ω_r : rotor angular electrical speed.

For a squirrel cage induction machine, as in the case of this paper, *vqr* and *vdr* in (3) and (4) are set to zero. An induction machine model can be represented with five differential equations as shown. To solve these equations, they have to be rearranged in the state-space form, In this case, state-space form can be achieved by inserting (5) and (6) in (1–4) and collecting the similar terms together so that each state derivative is a function of only other state variables and model inputs. Then, the modeling equations (1-4) of a squirrel cage induction motor in state-space become

$$\frac{dF_{qs}}{dt} = \omega_b \left[v_{qs} - \frac{\omega_e}{\omega_b} F_{ds} + \frac{R_s}{x_{ls}} \left(\frac{x^*_{ml}}{x_{lr}} F_{qr} + \left(\frac{x^*_{ml}}{x_{ls}} - 1 \right) F_{qs} \right) \right] \quad (13)$$

$$\frac{dF_{ds}}{dt} = \omega_b \left[v_{ds} + \frac{\omega_e}{\omega_b} F_{qs} + \frac{R_s}{x_{ls}} \left(\frac{x^*_{ml}}{x_{lr}} F_{dr} + \left(\frac{x^*_{ml}}{x_{ls}} - 1 \right) F_{ds} \right) \right] \quad (14)$$

$$\frac{dF_{qr}}{dt} = \omega_b \left[-\frac{(\omega_e - \omega_r)}{\omega_b} F_{dr} + \frac{R_r}{x_{lr}} \left(\frac{x^*_{ml}}{x_{ls}} F_{qs} + \left(\frac{x^*_{ml}}{x_{lr}} - 1 \right) F_{qr} \right) \right] \quad (15)$$

$$\frac{dF_{dr}}{dt} = \omega_b \left[\frac{(\omega_e - \omega_r)}{\omega_b} F_{qr} + \frac{R_r}{x_{lr}} \left(\frac{x^*_{ml}}{x_{ls}} F_{ds} + \left(\frac{x^*_{ml}}{x_{lr}} - 1 \right) F_{dr} \right) \right] \quad (16)$$

$$\frac{d\omega_r}{dt} = \left(\frac{p}{2J} \right) (T_e - T_L) \quad (17)$$

4.Matlab/Simulink Model & SIMULATION Results

Here simulation is carried out for two cases. In case I conventional three phase three level induction motor is simulated and in case II proposed multilevel drive is simulated.

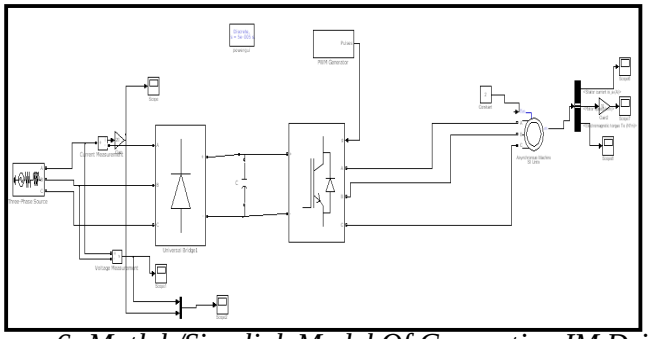

Figure6 :Matlab/Simulink Model Of Convention IM Drive

Fig. 6 shows the Matlab/Simulink model of conventional three phase three level induction motor drive. It consists of front end rectifier followed by three phase inverter.

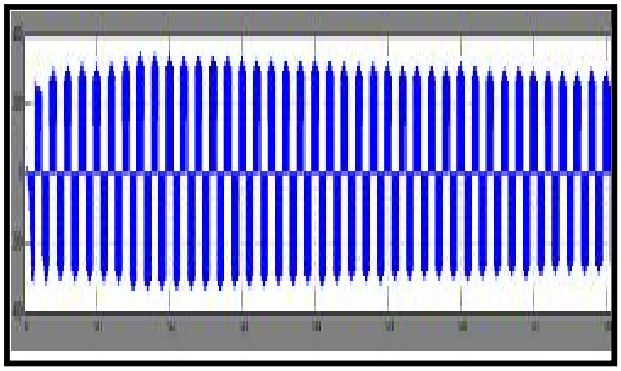

Figure7: Three Level Output

Fig. 7 shows the three level output of the conventional inverter. Her switching frequency is taken as 1050 hz.

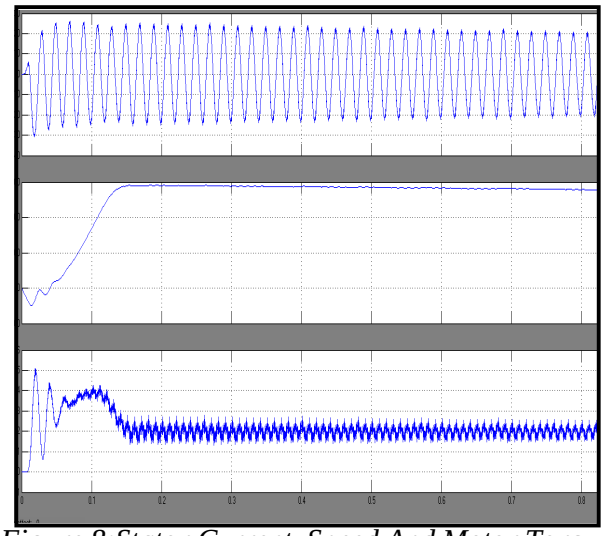

Figure 8:Stator Current, Speed And Motor Torque

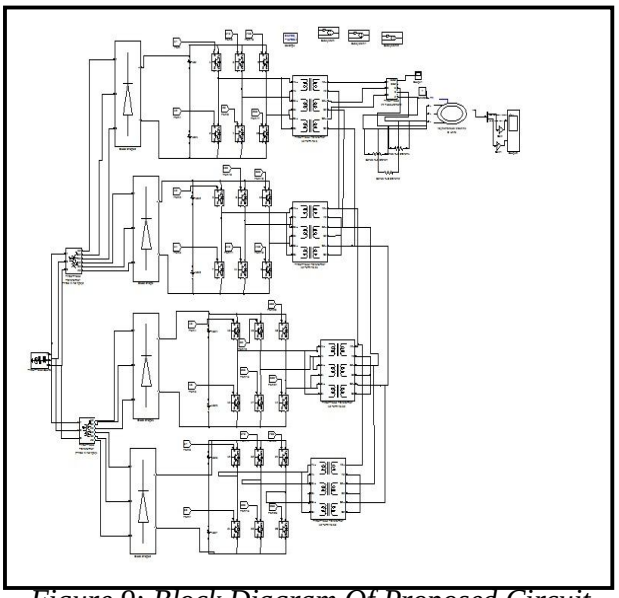

Figure 9: Block Diagram Of Proposed Circuit

Fig. 9 shows the block diagram of proposed series connected multilevel inverter fed induction motor drive. It consists of four inverters. Here we are using phase shifted carrier PWM.

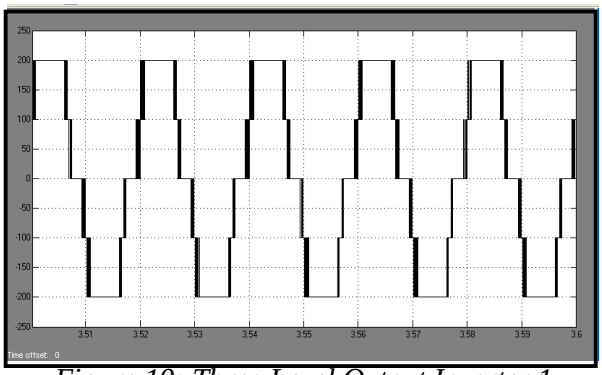

Figure 10: Three Level Output Inverter 1

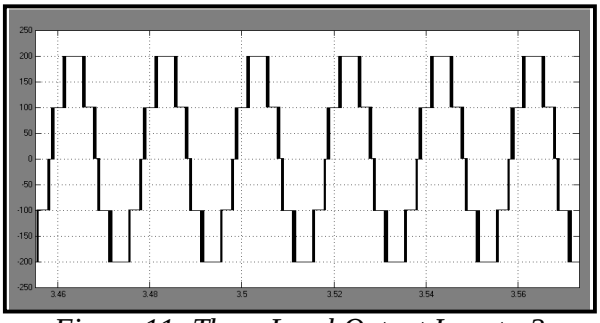

Figure 11: Three Level Output Inverter2

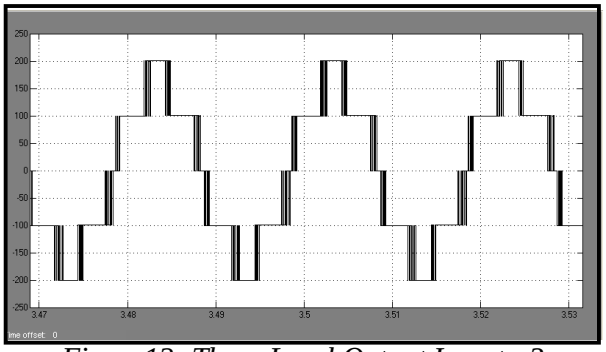

Figure12: Three Level Output Inverter3

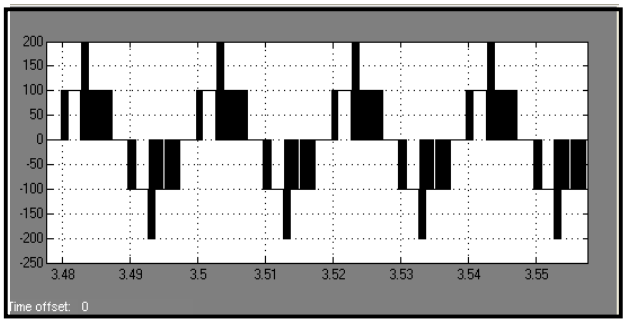

Figure13 :Three Level Output Inverter4

Fig10 to 13 shows the individual inverter outputs. From the figures it is clear that each output consists of only three levels.

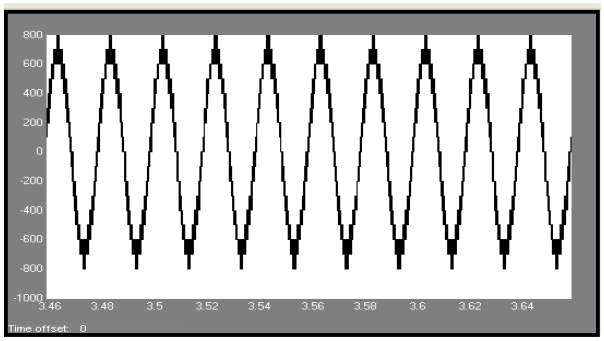

Figure14: Multilevel Output

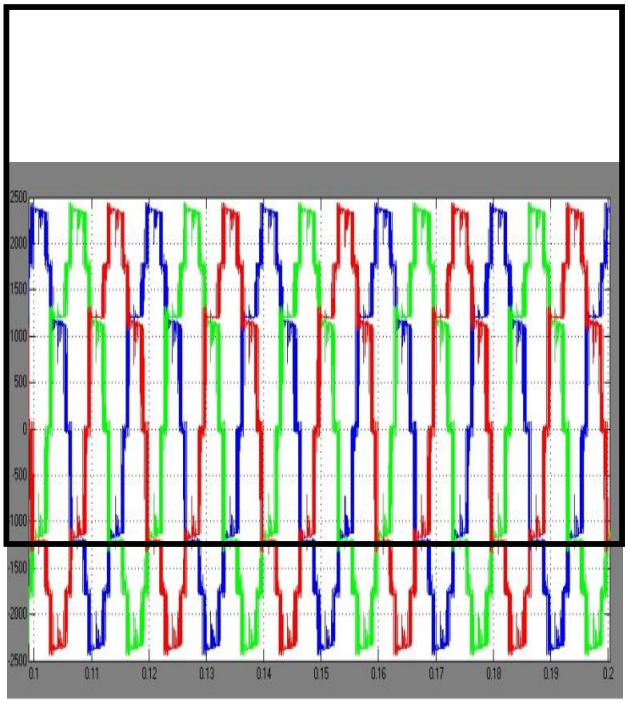

Figure15:Multilevel Output Three Phase

This waveform represents the output voltage of the three phase multilevel inverter.

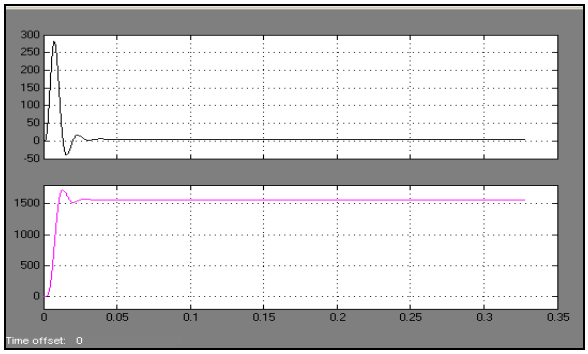

Figure16:Electromagnetic Torque And Speed Curves Of SQCIM

The first waveform represents the Electromagnetic Torque and rotor speed characteristics of the Squirrel cage Induction motor

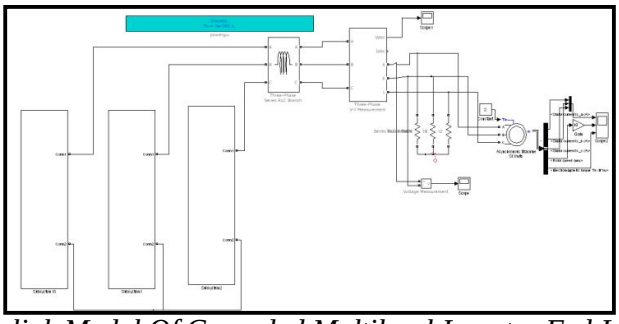

Figure17: Simulink Model Of Cascaded Multilevel Inverter Fed Induction Motor

Fig.17 shows the simulink model of the Cascaded multilevel inverter fed to an induction motor.

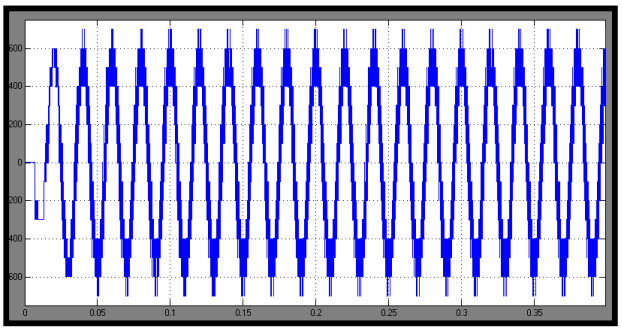

Figure18: Line Voltages Of Inverter

Fig.18 shows the line-line voltages of the CMLI

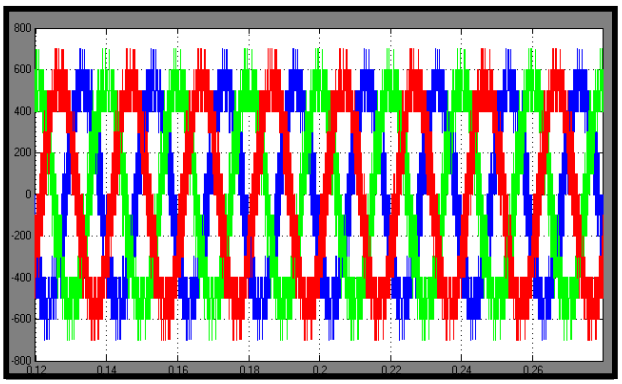

Figure19 :Three Phase Voltage Of Inverter

Fig.19 shows the three phase voltages of the CMLI

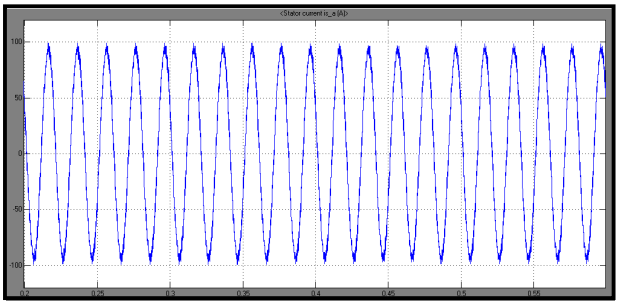

Figure20:Stator Current

Fig.20 shows the stator current characteristics of the induction motor.

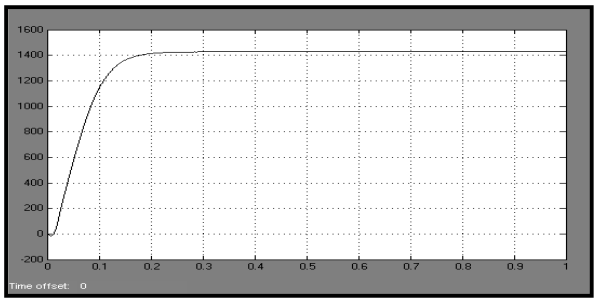

Figure21:Speed Of The Motor

Fig.21shows the speed curve of the induction motor. It is having the speed of 1450 r.p.m.

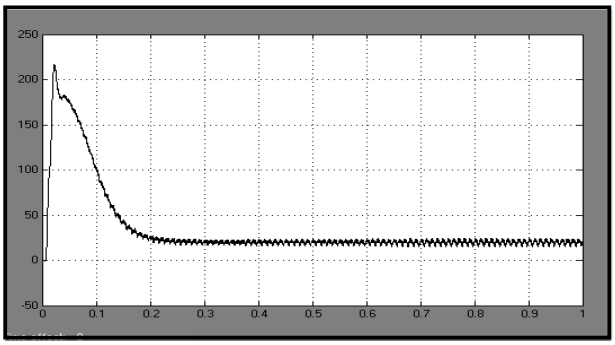

Figure22: Electromagnetic Torque

Fig.22 shows the electromagnetic torque characteristics of the induction motor.

5.Conclusion

A simulation model of systems consisting of a multilevel inverter and an induction machined has been developed a series connection of three-level inverters has been proposed for a medium-voltage SQIM drive with increased voltage capacity. The topology ensured high-power operations with medium-voltage output having several voltage levels. The reduction in the ratings of the dc bus capacitor and reduced

imbalance problems in the dc bus are some of the advantages of the proposed topology over the existing topologies. The disadvantage of the proposed topology is that it requires additional output transformers which introduce additional cost and losses. However, these transformers do not have complex underutilized windings like that required in cascaded H-bridge topologies. In this paper conventional and the cascaded multilevel inverter topologies were discussed and results were placed. Finally a Matlab/Simulink model is developed and simulation results are presented.

6.Reference

1. F. Wang, “Motor shaft voltages and bearing currents and their reduction in multilevel medium-voltage PWM voltage-source-inverter drive applications,” IEEE Trans. Ind. Appl., vol. 36, no. 5, pp. 1336–1341, Sep./Oct. 2000.
2. S. Chen and T. A. Lipo, “Bearing currents and shaft voltages of an induction motor under hard- and soft-switching inverter excitation,” IEEE Trans. Ind. Appl., vol. 34, no. 5, pp. 1042–1048, Sep./Oct. 1998.
3. L. M. Tolbert, F. Z. Peng, and T. G. Habetler, “Multilevel converters for large electric drives,” IEEE Trans. Ind. Appl., vol. 35, no. 1, pp. 36–44, Jan./Feb. 1999.
4. A.Muetze and A. Binder, “Calculation of circulating bearing currents in machines of inverter-based drive systems,” IEEE Trans. Ind. Electron., vol. 54, no. 2, pp. 932–938, Apr. 2007.
5. J. Rodriguez, J. S. Lai, and F. Z. Peng, “Multilevel inverters: A survey of topologies, control and applications,” IEEE Trans. Power Electron., vol. 49, no. 4, pp. 724–738, Aug. 2002.
6. P.W. Hammond, “A new approach to enhanced power quality for medium voltage drives,” IEEE Trans. Ind. Appl., vol. 33, no. 1, pp. 202–208, Jan./Feb. 1997.
7. R. Teodorescu, F. Blaabjerg, J. K. Pederson, E. Cengelci, and P. N. Enjeti, “Multilevel inverter by cascading industrial VSI,” IEEE Trans. Ind. Electron., vol. 49, no. 4, pp. 832–838, Aug. 2002.
8. A.Nabae, I. Takahashi, and H. Akagi, “A new neutral point clamped inverter,” IEEE Trans. Ind. Appl., vol. 17, no. 5, pp. 518–523, Sep./Oct. 1981.
9. J.-S. Lai and F. Z. Peng, “Multilevel converters—A new breed of power converters,” IEEE Trans. Ind. Appl., vol. 32, no. 3, pp. 509–517, May/Jun. 1996.
10. G. Cararra, S. Gardella, M. Marchesoni, R. Salutari, and G. Sciutto, “A new multilevel PWMmethod: A theoretical analysis,” IEEE Trans. Power Electron., vol. 7, no. 3, pp. 497–505, Jul. 1992.
11. A.M. Trzynadlowski, R. L. Kirlin, and S. Legowski, “Space vector PWM technique with minimum switching losses,” IEEE Trans. Ind. Electron., vol. 44, no. 2, pp. 173–181, Apr. 1997.

12. Y. S. Lai and S. R. Bowes, "Optimal bus-clamped PWM techniques for three-phase motor drives," in Proc. Annu. Conf. IEEE Ind. Electron. Soc., Busan, Korea, Nov. 2–6, 2004, pp. 1475–1480.
13. Suvajit Mukherjee and Gautam Poddar "A Series-Connected Three-Level Inverter Topology for Medium-Voltage Squirrel-Cage Motor Drive Applications" Ieee Transactions On Industry Applications, Vol. 46, No. 1, January/February 2010.